Received: 18 February 2024 | Revised: 23 May 2024 | Accepted: 3 July 2024

DOI: 10.1002/rnc.7535

RESEARCH ARTICLE

WILEY

Event-triggered consensus tracking strategy for data-driven multi-agent systems under DoS attacks

Jinliang Liu[1] | **Yipeng Liu**[2] | **Lijuan Zha**[3] | **Engang Tian**[4] | **Xiangpeng Xie**[5]

[1]School of Computer Science, Nanjing University of Information Science and Technology, Nanjing, China

[2]College of Information Engineering, Nanjing University of Finance and Economics, Nanjing, China

[3]College of Science, Nanjing Forestry University, Nanjing, China

[4]School of Optical-Electrical and Computer Engineering, University of Shanghai for Science and Technology, Shanghai, China

[5]Institute of Advanced Technology, Nanjing University of Posts and Telecommunications, Nanjing, China

Correspondence
Lijuan Zha, Nanjing Forestry University, Nanjing 210037, China.
Email: zhalijuan@vip.163.com

Funding information
National Natural Science Foundation of China, Grant/Award Numbers: 62373252, 62273174, 61903182; Natural Science Foundation of Jiangsu Province of China, Grant/Award Number: BK20230063; Startup Foundation for Introducing Talent of NUIST

Abstract

In this article, the event-triggered data-driven consensus problem is studied for multi-agent systems (MASs) with switching topologies under denial-of-service (DoS) attacks. Based on the model-free adaptive control (MFAC) approach, the controller is only correlated with the input/output (I/O) data of agents instead of the specific system model. First, the pseudo partial derivative (PPD) is employed to dynamically linearize the system model. Second, to save network bandwidth, an event-triggered scheme is introduced according to the I/O measurement and the output estimated error. Third, an attack compensation mechanism is adopted for the purpose of reducing the influence of DoS attacks. Then, a data-driven controller is designed to make the agents approach the desired trajectory on the basis of the estimation value of PPD. Moreover, by utilizing the Lyapunov stability theory, the tracking error is demonstrated to be convergent and the reliability of the controller is investigated. Finally, an example is simulated to verify the effectiveness of the consensus tracking strategy.

KEYWORDS

consensus tracking, data-driven, denial-of-service (DoS) attacks, model-free adaptive control (MFAC), multi-agent systems (MASs), pseudo partial derivative (PPD)

1 | INTRODUCTION

Nowadays, multi-agent systems (MASs) have been applied in a number of areas, such as robotic systems,[1] unmanned aerial vehicles[2] and autonomous underwater vehicles.[3] The tracking consensus problem for MASs is a basic research topic and has gained a lot of attention for the wide application of MASs,[4–6] which ensures that all agents achieve the same predefined trajectory finally with minimal control costs. For instance, the consensus problem for nonlinear MASs was investigated in Reference 4 with the consideration of sensor uncertainty. The authors in Reference 5 dealt with the consensus problem for heterogeneous MASs considering delays and noises. In Reference 6, a distributed robust controller was designed to solve the optimal output consensus issue for MASs. In the above results on tracking consensus problem, the dynamics of agents in MASs are presented with given models. However, constructing an accurate model of the system is often difficult due to the complexity in practice such as the nonlinear MASs. As a result, data-driven approaches have been proposed for MASs with unknown dynamics.[7,8]

As a novel data-driven approach, model-free adaptive control (MFAC) is an efficient control method for nonlinear systems, which can dynamically linearize the unknown system with the pseudo partial derivative (PPD).[9] For example, in Reference 10, a distributed MFAC approach was presented for the consensus control of MASs with switching topologies, where the input/output (I/O) measurement data of MASs is used to estimate the PPD. In Reference 11, a consensus tracking mechanism for discrete-time MASs was provided and the PPD can be derived by the input and saturated output measurement. Reference 12 theoretically analyzed the stability for MFAC-based MASs in the case where the tracking error was the monotonic convergence. In the MFAC approach, the PPD is independent of the specific system model and is estimated based on the I/O measurement data. In this article, the consensus problem for MASs is investigated by utilizing the MFAC method.

As is known, the communication network is applied to transmit control signals, which increases the efficiency and flexibility of the system. However, communication network can also bring negative effects on the system performance because of the constraint of bandwidth. To solve this problem, the event-triggered mechanism is recognized as an excellent choice for signal transmission.[13–15] Under an event-triggered mechanism, if the difference between the current sampled data and its previous transmitted data does not exceed a predefined threshold, then the current sampled data is not transmitted. For instance, in Reference 16, the event-triggered backstepping control issue was investigated for nonlinear strict-feedback systems. According to the adaptive output feedback backstepping method, Reference 17 discussed an event-triggered decentralized control problem for nonlinear large-scale interconnected systems. Extensive research has been conducted on MASs with event-triggered mechanisms. For example, in Reference 18, an event-triggered scheme was adopted for fault tolerant control in heterogeneous linear MASs. Reference 19 designed a distributed event-triggered mechanism to solve the consensus control problem for linear MASs. In Reference 20, Zhang and Tong devised a dynamic event-triggered mechanism for tracking control in nonlinear MASs. Based on MFAC, Reference 21 presented an event-triggered control strategy for discrete-time MASs.

With the implementation of communication network, the security problem of MASs under cyber attacks becomes another critical challenge in MASs.[22–25] Among various cyber attacks, denial-of-service (DoS) attacks can affect the system performance seriously since DoS attacks interrupt transmission by consuming the bandwidth resources.[26] Recently, the security control problem for MASs under DoS attacks has attracted intensive research. For instance, the researchers in Reference 27 investigated the consensus issue for MASs subject to DoS attacks with input saturation. Reference 28 designed a fault-tolerant controller to solve the resilient observer-based control issue for MASs under DoS attacks. However, the consensus problem for MAFC-based MASs subject to DoS attacks has not been fully investigated, which inspires our study in this work.

In traditional MASs, the communication relationships between agents are designed to be unchangeable. With the application of MASs on mobile devices, the relationships between agents change dynamically with time.[29–31] In recent years, the consensus issue for MASs with switching topologies has received massive attention. For example, in Reference 32, the bipartite consensus problem for MASs under random switching topologies was studied. Reference 33 studied the leader-following consensus problem of higher order MASs with variable typologies. Note that the results about the control approaches for network-bandwidth-limited MASs with switching topologies and DoS attacks are still few, how to solve this issue is an open research orientation.

Motivated by the mentioned works, the event-based consensus problem for a type of data-driven MASs with switching topologies and DoS attacks is studied in this article. In the homogeneous MAS, we design a controller by using the event-triggered model-free adaptive control (ETMFAC) approach to control the output of each agent to track the desired trajectory. The main contributions of this article are outlined as follows. (1) The framework of the event-triggered consensus issue for MASs under DoS attacks is constructed, in which the MFAC method is applied to dynamically linearize the unknown dynamics of agents with PPD. (2) An event-triggered mechanism and an attack compensation scheme are adopted to alleviate the impact of bandwidth limitation and DoS attacks in our framework. (3) A data-driven controller is introduced to make the agents approach the desired trajectory and the stability of the controller is verified by utilizing the Lyapunov stability theory.

The remainder of this article is indicated as below. First, the data-driven MAS model is established and the secure event-triggered model-free adaptive control (ETMFAC) approach is provided in Section 2. Then, in Section 3, the tracking performance of the MAS using the proposed secure ETMFAC approach is analyzed. Furthermore, an example is simulated in Section 4 to prove the validity of the proposed consensus control method for MASs with switching topologies. Finally, Section 5 concludes the article.

2 PROBLEM FORMULATION

2.1 System modeling

We consider a discrete-time MAS containing N homogeneous agents with switching topologies and the communication relationships among agents can be described as a directed graph $\mathcal{T}(\kappa)$ switched with time κ. As everyone knows, the aim of the consensus control problem is to make the trajectory of each agent consistent. For simplicity, a virtual leader indexed by 0 is introduced to generate the desired trajectory in our work. Then, the directed communication graph $\mathcal{T}(\kappa)$ among agents at time κ is detailed as $\mathcal{T}(\kappa) = (\mathcal{V} \cup \{0\}, \mathcal{E}(\kappa), \mathcal{A}(\kappa), \overline{\mathcal{E}}(\kappa), \mathcal{D}(\kappa))$. $\mathcal{V} = \{1, 2, \ldots, N\}$ is the set of N homogeneous agents and $\mathcal{V} \cup \{0\}$ represents the node set composed by N agents and the virtual leader 0. $\mathcal{E}(\kappa) \subseteq \mathcal{V} \times \mathcal{V}$ represents the set of communication edges among N agents at time κ. If agent j can receive messages from agent i, then $(i, j) \in \mathcal{E}(\kappa)$, agent i is the neighbor of agent j. Moreover, $\mathcal{A}(\kappa) = (a_{i,j}(\kappa))_{N\times N}$ denotes the adjacency matrix of $\mathcal{E}(\kappa)$, where $a_{i,j}(\kappa) = 1$ if $(i, j) \in \mathcal{E}(\kappa)$, otherwise $a_{i,j}(\kappa) = 0$ and $a_{i,i}(\kappa) = 0$. Additionally, $\overline{\mathcal{E}}(\kappa) \subseteq \{0\} \times \mathcal{V}$ is defined as the set of edges between the virtual leader and the agents. In matrix $\mathcal{D}(\kappa) = (d_i(\kappa))_{1\times N}$, $d_i(\kappa)$ is the corresponding relationship between agent i and the virtual leader. If agent i can acquire the desired trajectory, then $(0, i) \in \overline{\mathcal{E}}(\kappa)$ and $d_i(\kappa) = 1$, else $(0, i) \notin \overline{\mathcal{E}}(\kappa)$ and $d_i(\kappa) = 0$. Except that the node set $\mathcal{V} \cup \{0\}$ is independent of time κ since the agents in MAS are fixed without considering the fault, the rest elements in $\mathcal{T}(\kappa)$ will change over time. Suppose $\mathcal{T}(\kappa) \in \{\mathcal{T}_1, \mathcal{T}_2, \ldots, \mathcal{T}_X\}$, where $\{\mathcal{T}_1, \mathcal{T}_2, \ldots, \mathcal{T}_X\}$ is the set of all the possible communication graphs and X is the total number of the possible communication graphs. Define $\delta(\kappa) \in \{1, 2, \ldots, X\}$ as the switching signal, if $\delta(\kappa) = n$, there is $\mathcal{T}(\kappa) = \mathcal{T}_n$. Moreover, define $\mathcal{M}(\kappa) = \mathcal{C}(\kappa) - \mathcal{A}(\kappa)$ as the Laplacian matrix of $\mathcal{T}(\kappa)$, where $\mathcal{C}(\kappa) = diag\{c_1(\kappa), c_2(\kappa), \ldots, c_N(\kappa)\}$ and $c_i(\kappa)$ is the in-degree of vertex i, that is, $c_i(\kappa) = \sum_{j=1}^{N} a_{j,i}(\kappa)$.

Without loss of generality, the consensus tracking control framework of agent i ($\forall i \in \{1, 2, \ldots, N\}$) is presented in Figure 1. In Figure 1, the unknown dynamics of agent i can be presented as bellow:

$$r_i(\kappa + 1) = g_i(r_i(\kappa), v_i(\kappa)), \tag{1}$$

where $r_i(\kappa) \in R$ is the output signal, $r_d(\kappa)$ is the desired trajectory from a virtual leader, $v_i(\kappa) \in R$ is the input signal of agent i at time κ, and $g_i(\cdot)$ is an unknown nonlinear function.

For the convenience of the study, two assumptions are provided for nonlinear systems (1).

Assumption 1. The partial derivative of $g_i(\cdot)$ relating to $v_i(\kappa)$ is continuous.

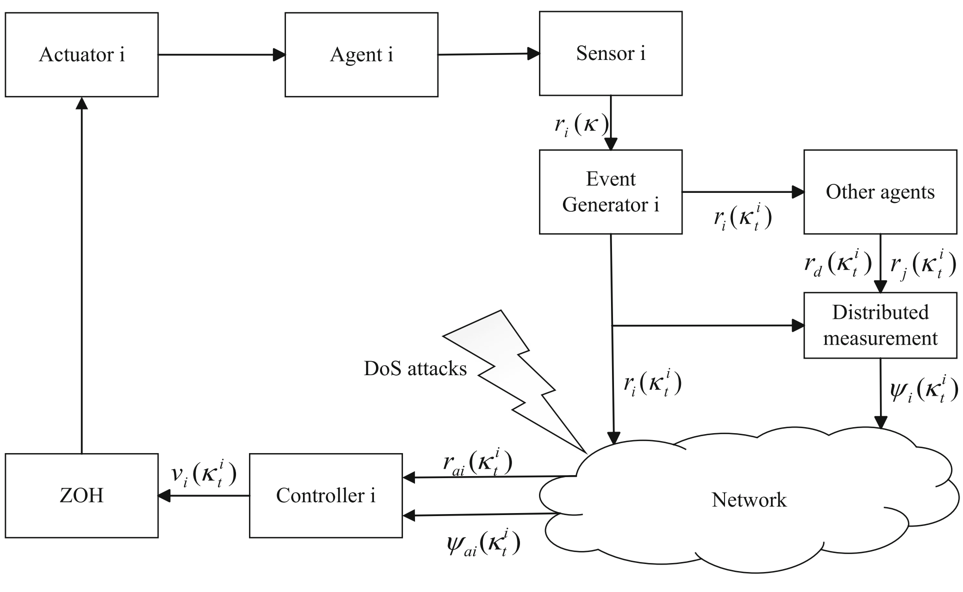

FIGURE 1 The framework of agent i in the tracking control system.

Assumption 2. In nonlinear system (1), the generalized Lipschitz condition is satisfied, in other words, if $\Delta v_i(\kappa) \neq 0$, then $|\Delta r_i(\kappa+1)| \leq b|\Delta v_i(\kappa)|$ holds for any κ, where $\Delta r_i(\kappa+1) = r_i(\kappa+1) - r_i(\kappa)$, $\Delta v_i(\kappa+1) = v_i(\kappa+1) - v_i(\kappa)$, $\Delta v_i(\kappa)$ is bounded and b is a positive constant.[34]

Remark 1. The two assumptions above are introduced for the dynamical linearization of the MAS. Assumption 1 is a general situation of the MFAC method. From Assumption 2, the change rate of $r_i(\kappa)$ lies on $\Delta v_i(\kappa)$. Therefore, the input difference $\Delta v_i(\kappa)$ is bounded, then the output difference $\Delta r_i(\kappa)$ is also bounded.

Lemma 1 (35). *Consider that system (1) satisfies Assumption 1 and 2, when $\Delta v_i(\kappa) \neq 0$ holds, the following dynamic model (2) can be derived according to system (1)*:

$$\Delta r_i(\kappa+1) = \omega_i(\kappa)\Delta v_i(\kappa), \tag{2}$$

where $\omega_i(\kappa)$ is bounded and $|\omega_i(\kappa)| \leq b$.

In Lemma 1, system (1) is linearized as an MFAC-based system with a PPD parameter $\omega_i(\kappa)$, which is data-driven with the I/O measurement data instead of a specific model. Then, a corresponding controller i is designed to generate the input signal $v_i(\kappa)$ for the agent i. The general model of any controller i to be constructed is given as follows:

$$v_i(\kappa) = g_i'(r_i(\kappa), \psi_i(\kappa)), \tag{3}$$

where $g_i'(\cdot)$ is an unknown function and $\psi_i(\kappa)$ is the combined measurement error defined to be later. The major purpose is to design a data-driven controller for each agent to approach the desired trajectory. The combined measurement error is given as follows:

$$\psi_i(\kappa) = \sum_{j\in N_i(\kappa)} a_{j,i}(\kappa)(r_j(\kappa) - r_i(\kappa)) + d_i(\kappa)(r_d(\kappa) - r_i(\kappa)), \tag{4}$$

where $N_i(\kappa) = \{j \in \mathcal{V} | (j,i) \in \mathcal{E}(\kappa)\}$ is the neighbor set of the agent i at time κ.

Remark 2. In this article, we assume there is a directed spanning tree rooting from the virtual leader, which implies that each agent can acquire the desired trajectory from either the virtual leader or neighbor agents. In other words, in Equation (4), $a_{j,i}(\kappa)$ and $d_i(\kappa)$ are not zero at the same time, and the combined measurement error $\psi_i(\kappa)$ is not zero, otherwise the agents cannot get the investigation information.

2.2 | Event-triggered scheme

To reduce the transmission of similar data, an event-triggered generator is set to selectively transmit the output $r_i(\kappa)$ from agent i in Figure 1. Suppose $r_i(\kappa)$ is the current sampled output and $r_i(\kappa_t^i)$ is the last triggered output. When the event-triggered condition is satisfied, the current output $r_i(\kappa)$ can be transmitted into the network. κ_t^i is the tth triggered time instant for agent i, which is the nearest triggered time instant to current time κ. If $r_i(\kappa)$ is triggered out, the time instant κ is the $(t+1)$th triggered time instant for agent i, that is, $\kappa_{t+1}^i = \kappa$

$$\Upsilon(r_i(\kappa_t^i) - r_i(\kappa)) > \frac{\sqrt{\gamma(1-4(1+Q_i)^2)}}{2|Q_i|}|\varepsilon_i(\kappa)|, \tag{5}$$

where $\Upsilon(\cdot)$ is defined as the function about the difference between $r_i(\kappa_t^i)$ and $r_i(\kappa)$.

In the event-triggered condition (5), $0 < \gamma < 1$ is a constant, Q_i is the parameter which satisfies $0 < 1 - 4(1+Q_i)^2 < 1$, $\varepsilon_i(\kappa)$ is the output estimated error given as below:

$$\varepsilon_i(\kappa) = r_i(\kappa) - \hat{r}_i(\kappa), \tag{6}$$

where $\hat{r}_i(\kappa)$ is the estimation value of $r_i(\kappa)$.

The output evaluation function is used to estimate the output value $r_i(\kappa)$ at time κ and is given as follows:

$$\hat{r}_i(\kappa+1) = \hat{r}_i(\kappa) + \hat{\omega}_i(\kappa)\Delta\nu_i(\kappa_t^i) + Q_i(\hat{r}_i(\kappa) - r_i(\kappa_t^i)), \tag{7}$$

where $\hat{\omega}_i(\kappa)$ is the estimation value of the PPD parameter $\omega_i(\kappa)$. Additionally, $\Delta\nu_i(\kappa_t^i) = \nu_i(\kappa_t^i) - \nu_i(\kappa_t^i - 1)$ is the difference between the system input at κ_t^i and the input at the prior sampled time instant before κ_t^i.

Moreover, the expression for the function $\Upsilon(\cdot)$ is given as follows:

$$\Upsilon(r_i(\kappa_t^i) - r_i(\kappa)) = \begin{cases} |r_i(\kappa_t^i) - r_i(\kappa)|, & if \quad |\varepsilon_i(\kappa)| > \zeta_i, \\ 0, & otherwise, \end{cases} \tag{8}$$

where ζ_i is the bound of $\varepsilon_i(\kappa)$ which will be designed in the subsequent chapter. Additionally, based on Equation (4), $\psi_i(\kappa_t^i)$ is defined as the combined measurement error at the triggered time.

Remark 3. Combining the event-triggered condition (5) and Equation (8), it is worth noting that if $|\varepsilon_i(\kappa)| \le \zeta_i$, then $\Upsilon(r_i(\kappa_t^i) - r_i(\kappa)) = 0$, which implies that the condition (5) is not satisfied and the event generator will not be triggered. Therefore, the parameter ζ_i of $\Upsilon(\cdot)$ is adjustable to control the number of event-triggered instants. For example, if the value of ζ_i increases, then the sampled data satisfying the inequality $|\varepsilon_i(\kappa)| > \zeta_i$ will decrease, so the number of the event-triggered instants will ultimately decrease.

2.3 | Dos attacks model

As illustrated in Figure 1, the triggered output $r_i(\kappa_t^i)$ and the the combined measurement error $\psi_i(\kappa_t^i)$ for agent i at the triggered time κ_t^i are both transmitted to the controller i. Assume that the network is faced with DoS attacks, which aim to block transmission and destroy the system's performance.

In this article, a Bernoulli variable $\beta_i(\kappa_t^i) \in \{0, 1\}$ is introduced to denote whether DoS attack occurs (or not). The probabilities of DoS attacks occurring or not at the triggered time instant κ_t^i are presented as follows[29]:

$$\begin{cases} P\{\beta_i(\kappa_t^i) = 0\} = 1 - \overline{\beta}_i, \\ P\{\beta_i(\kappa_t^i) = 1\} = \overline{\beta}_i. \end{cases} \tag{9}$$

Thus, the triggered output $r_i(\kappa_t^i)$ and the combined measurement error $\psi_i(\kappa_t^i)$ under DoS attacks are $\overline{r}_{ai}(\kappa_t^i)$ and $\overline{\psi}_{ai}(\kappa_t^i)$:

$$\overline{r}_{ai}(\kappa_t^i) = \beta_i(\kappa_t^i) r_i(\kappa_t^i),$$

$$\overline{\psi}_{ai}(\kappa_t^i) = \beta_i(\kappa_t^i) \psi_i(\kappa_t^i).$$

For the purpose of addressing the problem of DoS attacks, an attack compensation scheme is given as follows:

$$\begin{aligned} r_{ai}(\kappa_t^i) &= \beta_i(\kappa_t^i) r_i(\kappa_t^i) + (1 - \beta_i(\kappa_t^i)) r_i(\kappa_{t-1}^i), \\ \psi_{ai}(\kappa_t^i) &= \beta_i(\kappa_t^i) \psi_i(\kappa_t^i) + (1 - \beta_i(\kappa_t^i)) \psi_i(\kappa_{t-1}^i). \end{aligned} \tag{10}$$

Remark 4. As shown in the attack compensation scheme (10), when $\beta_i(\kappa_t^i) = 0$, the triggered output $r_i(\kappa_t^i)$ and the combined measurement error $\psi_i(\kappa_t^i)$ are blocked by DoS attacks, and the inputs of the controller i will be updated by the last effective values $r_i(\kappa_{t-1}^i)$ and $\psi_i(\kappa_{t-1}^i)$ for the compensation of DoS attacks.

Remark 5. Both of the two network-induced phenomena DoS attacks and packet dropouts can lead to unsuccessful transmissions, but they are different. The DoS attacks addressed in this article is maliciously launched by the attackers to block the signal exchange between the agents, while packet dropouts are caused by network congestion. Nowadays, some DoS attacks detection method (see References 36 and 37 for example) have been proposed, by which one can know whether or not the DoS attacks are in presence.

2.4 Design of the controller based on ETMFAC method

In this article, the dynamic linearization approach can be used for each agent on the basis of the PPD parameter $\omega_i(\kappa)$. Since it is difficult to get the exact value of $\omega_i(\kappa)$, $\hat{\omega}_i(\kappa)$ is used to estimate the value of the PPD parameter $\omega_i(\kappa)$. The performance index function $S_1[\hat{\omega}_i(\kappa)]$ is given by using the time-varying parameter estimation method[38] to get $\hat{\omega}_i(\kappa)$. The function $S_1[\hat{\omega}_i(\kappa)]$ is presented as follows:

$$S_1[\hat{\omega}_i(\kappa)] = (\Delta r_i(\kappa) - \hat{\omega}_i(\kappa)\Delta v_i(\kappa-1))^2 + \mu(\hat{\omega}_i(\kappa) - \hat{\omega}_i(\kappa-1))^2, \tag{11}$$

where $\mu > 0$ is a weight factor.

Define the control input index function $S_2[v_i(\kappa)]$, then we use the MFAC method to design the controller. The function $S_2[v_i(\kappa)]$ is given as below:

$$S_2[v_i(\kappa)] = (\psi_i(\kappa) - \hat{\omega}_i(\kappa-1)\Delta v_i(\kappa))^2 + \lambda(v_i(\kappa) - v_i(\kappa-1))^2, \tag{12}$$

where $\lambda > 0$ is a weight factor.

From $S_1[\hat{\omega}_i(\kappa)]$ in Equation (11), one has:

$$S_1[\hat{\omega}_i(\kappa)] = (\Delta r_i(\kappa)^2 - 2\hat{\omega}_i(\kappa)\Delta r_i(\kappa)\Delta v_i(\kappa-1) + \hat{\omega}_i(\kappa)^2\Delta v_i(\kappa-1)^2) + \mu(\hat{\omega}_i(\kappa)^2 - 2\hat{\omega}_i(\kappa-1)\hat{\omega}_i(\kappa) + \hat{\omega}_i(\kappa-1)^2). \tag{13}$$

To minimize $S_1[\hat{\omega}_i(\kappa)]$, let $\frac{\partial S_1[\hat{\omega}_i(\kappa)]}{\partial \hat{\omega}_i(\kappa)} = 0$, it can be obtained that

$$-2\Delta r_i(\kappa)\Delta v_i(\kappa-1) + 2\Delta v_i(\kappa-1)^2\hat{\omega}_i(\kappa) + \mu(2\hat{\omega}_i(\kappa) - 2\hat{\omega}_i(\kappa-1)) = 0 \tag{14}$$

then one has

$$\begin{aligned}(\mu + \Delta v_i(\kappa-1)^2)\hat{\omega}_i(\kappa) &= \mu\hat{\omega}_i(\kappa-1) + \Delta r_i(\kappa)\Delta v_i(\kappa-1) \\ &= (\mu + \Delta v_i(\kappa-1)^2)\hat{\omega}_i(\kappa-1) + \Delta r_i(\kappa)\Delta v_i(\kappa-1) - \Delta v_i(\kappa-1)^2\hat{\omega}_i(\kappa-1).\end{aligned} \tag{15}$$

Hence, one can get

$$\hat{\omega}_i(\kappa) = \hat{\omega}_i(\kappa-1) + \frac{\Delta v_i(\kappa-1)\Delta r_i(\kappa) - \Delta v_i(\kappa-1)^2\hat{\omega}_i(\kappa-1)}{\mu + \Delta v_i(\kappa-1)^2}.$$

So as to enhance the flexibility and generality of the distributed MFAC approach, one has

$$\hat{\omega}_i(\kappa) = \hat{\omega}_i(\kappa-1) + \frac{\eta\Delta v_i(\kappa-1)(\Delta r_i(\kappa) - \hat{\omega}_i(\kappa-1)\Delta v_i(\kappa-1))}{\mu + \Delta v_i(\kappa-1)^2}, \tag{16}$$

where $\eta \in (0, 1]$ is the step size factor. To strengthen the tracking ability of the parameter estimation method in Equation (16) for time-varying parameters, define $\hat{\omega}_i(\kappa) = \hat{\omega}_i(1)$ if $|\Delta v_i(\kappa-1)| \le \alpha$, or $|\hat{\omega}_i(\kappa)| \le \alpha$, or $sign(\hat{\omega}_i(1)) \ne sign(\hat{\omega}_i(\kappa))$, where α is a sufficiently small constant and $\alpha > 0$, $\hat{\omega}_i(1)$ represents the initial value of $\hat{\omega}_i(\kappa)$.

Similarly, from $S_2[v_i(\kappa)]$ in Equation (12), it can be derived that:

$$\begin{aligned}S_2[v_i(\kappa)] &= (\psi_i(\kappa) - \hat{\omega}_i(\kappa-1)\Delta v_i(\kappa))^2 + \lambda(v_i(\kappa) - v_i(\kappa-1))^2 \\ &= (\psi_i(\kappa)^2 - 2\hat{\omega}_i(\kappa-1)\Delta v_i(\kappa)\psi_i(\kappa) + \hat{\omega}_i(\kappa-1)^2\Delta v_i(\kappa)^2) + \lambda(v_i(\kappa)^2 - 2v_i(\kappa)v_i(\kappa-1) + v_i(\kappa-1)^2) \\ &= \psi_i(\kappa)^2 - 2\hat{\omega}_i(\kappa-1)\psi_i(\kappa)(v_i(\kappa) - v_i(\kappa-1)) + \hat{\omega}_i(\kappa-1)^2(v_i(\kappa) - v_i(\kappa-1))^2 \\ &\quad + \lambda(v_i(\kappa)^2 - 2v_i(\kappa)v_i(\kappa-1) + v_i(\kappa-1)^2) \\ &= \psi_i(\kappa)^2 - 2\hat{\omega}_i(\kappa-1)\psi_i(\kappa)v_i(\kappa) + 2\hat{\omega}_i(\kappa-1)\psi_i(\kappa)v_i(\kappa-1) \\ &\quad + \hat{\omega}_i(\kappa-1)^2(v_i(\kappa)^2 - 2v_i(\kappa-1)v_i(\kappa) + v_i(\kappa-1)^2) + \lambda(v_i(\kappa)^2 - 2v_i(\kappa)v_i(\kappa-1) + v_i(\kappa-1)^2)\end{aligned}$$

then,

$$\begin{aligned}\frac{\partial S_2[v_i(\kappa)]}{\partial v_i(\kappa)} &= -2\hat{\omega}_i(\kappa-1)\psi_i(\kappa) + \hat{\omega}_i(\kappa-1)^2(2v_i(\kappa) - 2v_i(\kappa-1)) + \lambda(2v_i(\kappa) - 2v_i(\kappa-1)) \\ &= -2\hat{\omega}_i(\kappa-1)\psi_i(\kappa) + 2\hat{\omega}_i(\kappa-1)^2 v_i(\kappa) - 2\hat{\omega}_i(\kappa-1)^2 v_i(\kappa-1) + 2\lambda v_i(\kappa) - 2\lambda v_i(\kappa-1).\end{aligned} \tag{17}$$

To minimize $S_2[v_i(\kappa)]$, let $\frac{\partial S_2[v_i(\kappa)]}{\partial v_i(\kappa)} = 0$, it can be obtained that

$$(\hat{\omega}_i(\kappa-1)^2 + \lambda)(v_i(\kappa) - v_i(\kappa-1)) = \hat{\omega}_i(\kappa-1)\psi_i(\kappa) \tag{18}$$

$$v_i(\kappa) = v_i(\kappa-1) + \frac{\hat{\omega}_i(\kappa-1)\psi_i(\kappa)}{\lambda + \hat{\omega}_i(\kappa-1)^2}.$$

Also, Equation (17) below is utilized to enhance the flexibility and generality of the distributed MFAC method:

$$v_i(\kappa) = v_i(\kappa-1) + \frac{\rho\hat{\omega}_i(\kappa-1)\psi_i(\kappa)}{\lambda + \hat{\omega}_i(\kappa-1)^2}, \tag{19}$$

where $\rho \in (0, 1]$ is a factor representing the step size.

Then, on account of the influence of DoS attacks, the ETMFAC method is introduced as below.

$$\hat{\omega}_i(\kappa) = \begin{cases} \hat{\omega}_i(\kappa_t^i), & \kappa_t^i < \kappa < \kappa_{t+1}^i \\ \hat{\omega}_i(\kappa-1) + \frac{\eta\Delta v_i(\kappa-1)(r_{ai}(\kappa) - r_i(\kappa-1) - \hat{\omega}_i(\kappa-1)\Delta v_i(\kappa-1))}{\mu + \Delta v_i(\kappa-1)^2}, & \kappa = \kappa_t^i \end{cases}, \tag{20}$$

$$v_i(\kappa) = \begin{cases} v_i(\kappa_t^i), & \kappa_t^i < \kappa < \kappa_{t+1}^i \\ v_i(\kappa-1) + \frac{\rho\hat{\omega}_i(\kappa-1)}{\lambda + \hat{\omega}_i(\kappa-1)^2}\psi_{ai}(\kappa), & \kappa = \kappa_t^i \end{cases}. \tag{21}$$

The designed controller can be expressed as Eq. (21). If the output of agent i satisfies the event-triggered condition (5) at time κ, the signal of the controller $v_i(\kappa)$ is updated as $v_i(\kappa-1) + \frac{\rho\hat{\omega}_i(\kappa-1)}{\lambda + \hat{\omega}_i(\kappa-1)^2}\psi_{ai}(\kappa)$. Otherwise, the signal at the last event-triggered instant is utilized, that is, $v_i(\kappa) = v_i(\kappa_t^i)$.

Remark 6. From Equation (20) and Equation (21) above, we can derive that the PPD estimation and the design of the controller are dependent on the I/O signal of agents. Therefore, the ETMFAC approach is a data-driven control method to solve the consensus tracking issue of MASs.

3 | MAIN RESULTS

In this section, the convergence of the system tracking error will be demonstrated. First, the PPD estimation is proved to be bounded and the boundedness of the output estimated error is verified in Theorem 1 by using the Lyapunov stability theory. Then, the convergence of the tracking error is demonstrated in Theorem 2 on the basis of Theorem 1.

Theorem 1. *Based on Assumptions 1 and 2, for* $0 < \gamma < 1$, $0 < 1 - 4(1 + Q_i)^2 < 1$, *the PPD estimation* $\hat{\omega}_i(\kappa)$ *and the output estimated error* $\varepsilon_i(\kappa)$ *are bounded if the inequality holds as follows*:

$$4Q_i^2(r_i(\kappa_t^i) - r_i(\kappa))^2 \leq \gamma(1 - 4(1 + Q_i)^2)(\varepsilon_i(\kappa))^2.$$

Proof. First, the proof of the boundness of $\hat{\omega}_i(\kappa)$ is given.

Consider the case where $|\Delta v_i(\kappa-1)| > \alpha$ or $|\omega_i(\kappa)| > \alpha$, define $\overline{\omega}_i(\kappa)$ as the error between $\hat{\omega}_i(\kappa)$ and $\omega_i(\kappa)$, $\overline{\omega}_i(\kappa) = \hat{\omega}_i(\kappa) - \omega_i(\kappa)$.

If $\kappa_t^i = \kappa_{t-1}^i + 1$, there is no other time instants between κ_{t-1}^i and κ_t^i. For $\kappa = \kappa_t^i$, from Equation (10) and Equation (20), one has

$$\begin{aligned}
\hat{\omega}_i(\kappa) &= \hat{\omega}_i(\kappa-1) + \frac{\eta\Delta\nu_i(\kappa-1)}{\mu+\Delta\nu_i(\kappa-1)^2}(\beta_i(\kappa_t^i)r_i(\kappa_t^i) + (1-\beta_i(\kappa_t^i))r_i(\kappa_t^i-1) \\
&\quad - r_i(\kappa_t^i-1) - \hat{\omega}_i(\kappa-1)\Delta\nu_i(\kappa-1)) \\
&= \hat{\omega}_i(\kappa-1) + \frac{\eta\Delta\nu_i(\kappa-1)}{\mu+\Delta\nu_i(\kappa-1)^2}\beta_i(\kappa_t^i)\Delta r_i(\kappa_t^i) - \frac{\eta\Delta\nu_i(\kappa-1)^2}{\mu+\Delta\nu_i(\kappa-1)^2}\hat{\omega}_i(\kappa-1) \\
&= \hat{\omega}_i(\kappa-1) + \frac{\eta\Delta\nu_i(\kappa-1)}{\mu+\Delta\nu_i(\kappa-1)^2}\beta_i(\kappa_t^i)\Delta r_i(\kappa_t^i) - \frac{\eta\Delta\nu_i(\kappa-1)^2}{\mu+\Delta\nu_i(\kappa-1)^2}(\overline{\omega}_i(\kappa-1) + \omega_i(\kappa-1)) \\
&= \hat{\omega}_i(\kappa-1) + \frac{\eta\Delta\nu_i(\kappa-1)}{\mu+\Delta\nu_i(\kappa-1)^2}(\beta_i(\kappa_t^i)\Delta r_i(\kappa_t^i) - \omega_i(\kappa-1)\Delta\nu_i(\kappa-1)) - \frac{\eta\Delta\nu_i(\kappa-1)^2}{\mu+\Delta\nu_i(\kappa-1)^2}\overline{\omega}_i(\kappa-1) \\
&= \hat{\omega}_i(\kappa-1) + \frac{\eta\Delta\nu_i(\kappa-1)}{\mu+\Delta\nu_i(\kappa-1)^2}(\beta_i(\kappa_t^i)\Delta r_i(\kappa_t^i) - \Delta r_i(\kappa)) - \frac{\eta\Delta\nu_i(\kappa-1)^2}{\mu+\Delta\nu_i(\kappa-1)^2}\overline{\omega}_i(\kappa-1).
\end{aligned} \tag{22}$$

Then, based on the definition of $\overline{\omega}_i(\kappa)$, from Equation (22) it can be obtained that

$$\begin{aligned}
\overline{\omega}_i(\kappa) &= \frac{\eta\Delta\nu_i(\kappa-1)}{\mu+\Delta\nu_i(\kappa-1)^2}(\beta_i(\kappa_t^i)\Delta r_i(\kappa_t^i) - \Delta r_i(\kappa)) - \frac{\eta\Delta\nu_i(\kappa-1)^2}{\mu+\Delta\nu_i(\kappa-1)^2}\overline{\omega}_i(\kappa-1) + \hat{\omega}_i(\kappa-1) - \omega_i(\kappa) \\
&= -\frac{\eta\Delta\nu_i(\kappa-1)^2}{\mu+\Delta\nu_i(\kappa-1)^2}\overline{\omega}_i(\kappa-1) - \omega_i(\kappa) + \frac{\eta\Delta\nu_i(\kappa-1)}{\mu+\Delta\nu_i(\kappa-1)^2}\beta_i(\kappa_t^i)\Delta r_i(\kappa_t^i) - \frac{\eta\Delta\nu_i(\kappa-1)}{\mu+\Delta\nu_i(\kappa-1)^2}\Delta r_i(\kappa) + \hat{\omega}_i(\kappa-1) \\
&= -\frac{\eta\Delta\nu_i(\kappa-1)^2}{\mu+\Delta\nu_i(\kappa-1)^2}\overline{\omega}_i(\kappa-1) - \omega_i(\kappa) + \frac{\eta\Delta\nu_i(\kappa-1)}{\mu+\Delta\nu_i(\kappa-1)^2}\beta_i(\kappa_t^i)\omega_i(\kappa_t^i-1)\Delta\nu_i(\kappa_t^i-1) \\
&\quad - \frac{\eta\Delta\nu_i(\kappa-1)^2}{\mu+\Delta\nu_i(\kappa-1)^2}\omega_i(\kappa-1) + \hat{\omega}_i(\kappa-1).
\end{aligned}$$

Since $\overline{\omega}_i(\kappa-1) = \hat{\omega}_i(\kappa-1) - \omega_i(\kappa-1)$, one obtains

$$\begin{aligned}
\overline{\omega}_i(\kappa) &= -\frac{\eta\Delta\nu_i(\kappa-1)^2}{\mu+\Delta\nu_i(\kappa-1)^2}\overline{\omega}_i(\kappa-1) - \omega_i(\kappa) + \frac{\eta\Delta\nu_i(\kappa-1)}{\mu+\Delta\nu_i(\kappa-1)^2}\beta_i(\kappa_t^i)\omega_i(\kappa_t^i-1)\Delta\nu_i(\kappa_t^i-1) \\
&\quad - \frac{\eta\Delta\nu_i(\kappa-1)^2}{\mu+\Delta\nu_i(\kappa-1)^2}\omega_i(\kappa-1) + \overline{\omega}_i(\kappa-1) + \omega_i(\kappa-1) \\
&= (1 - \frac{\eta\Delta\nu_i(\kappa-1)^2}{\mu+\Delta\nu_i(\kappa-1)^2})\overline{\omega}_i(\kappa-1) - \omega_i(\kappa) + \frac{\eta\Delta\nu_i(\kappa-1)}{\mu+\Delta\nu_i(\kappa-1)^2}\beta_i(\kappa_t^i)\omega_i(\kappa_t^i-1)\Delta\nu_i(\kappa_t^i-1) \\
&\quad + (1 - \frac{\eta\Delta\nu_i(\kappa-1)^2}{\mu+\Delta\nu_i(\kappa-1)^2})\omega_i(\kappa-1).
\end{aligned} \tag{23}$$

According to Equation (23), take the absolute value of $\overline{\omega}_i(\kappa)$, we can get

$$\begin{aligned}
|\overline{\omega}_i(\kappa)| \leq{}& \left|1 - \frac{\eta\Delta\nu_i(\kappa-1)^2}{\mu+\Delta\nu_i(\kappa-1)^2}\right||\overline{\omega}_i(\kappa-1)| + \left|1 - \frac{\eta\Delta\nu_i(\kappa-1)^2}{\mu+\Delta\nu_i(\kappa-1)^2}\right||\omega_i(\kappa-1)| \\
&+ \left|\frac{\eta\Delta\nu_i(\kappa-1)}{\mu+\Delta\nu_i(\kappa-1)^2}\right|\left|\beta_i(\kappa_t^i)\omega_i(\kappa_t^i-1)\Delta\nu_i(\kappa_t^i-1)\right| + |\omega_i(\kappa)|.
\end{aligned} \tag{24}$$

It can be obtained that the function $\frac{\eta\Delta\nu_i(\kappa-1)^2}{\mu+\Delta\nu_i(\kappa-1)^2}$ is monotonically increasing for $\Delta\nu_i(\kappa-1)^2$. Since $|\Delta\nu_i(\kappa)| \neq 0$ and $|\Delta\nu_i(\kappa-1)| > \alpha$, it can be derived that $\frac{\eta\Delta\nu_i(\kappa-1)^2}{\mu+\Delta\nu_i(\kappa-1)^2} > \frac{\eta\alpha^2}{\mu+\alpha^2}$. When $0 < \eta \leq 1$, $\mu \geq 1$, one has the inequality as follows:

$$0 < \left|1 - \frac{\eta\Delta\nu_i(\kappa-1)^2}{\mu+\Delta\nu_i(\kappa-1)^2}\right| < 1 - \frac{\eta\alpha^2}{\mu+\alpha^2} \triangleq m_1 < 1. \tag{25}$$

In addition, one obtains

$$0 \leq \left| \frac{\eta \Delta \nu_i(\kappa-1)}{\mu + \Delta \nu_i(\kappa-1)^2} \right| < \frac{\eta \Delta \nu_i(\kappa-1)}{2\Delta \nu_i(\kappa-1)\sqrt{\mu}} = \frac{\eta}{2\sqrt{\mu}} \triangleq m_2 < 1, \tag{26}$$

where m_1, m_2 are constants. From Lemma 1, since $|\omega_i(\kappa)| \leq b$, the inequality (24) can be transformed into

$$\begin{aligned} |\overline{\omega}_i(\kappa)| &< m_1|\overline{\omega}_i(\kappa-1)| + b + m_1 b + m_2\overline{\beta}_i b\alpha \\ &< m_1(m_1|\overline{\omega}_i(k-2)| + b + m_1 b + m_2\overline{\beta}_i b\alpha) + b + m_1 b + m_2\overline{\beta}_i b\alpha \\ &< \cdots \\ &< m_1^{\kappa-1}|\overline{\omega}_i(1)| + (b + m_1 b + m_2\overline{\beta}_i b\alpha)\frac{1-m_1^{\kappa-1}}{1-m_1} \end{aligned} \tag{27}$$

which implies $\overline{\omega}_i(\kappa)$ is bounded, therefore, $\hat{\omega}_i(\kappa)$ is also bounded because of the boundedness of $\omega_i(\kappa)$.

If $\kappa_t^i \geq \kappa_{t-1}^i + 2$, for $\kappa_{t-1}^i \leq \kappa < \kappa_t^i$, from Equation (21) we have $\nu_i(\kappa_t^i - 1) = \nu_i(\kappa_t^i - 2) \cdots = \nu_i(\kappa) = \cdots = \nu_i(\kappa_{t-1}^i + 1) = \nu_i(\kappa_{t-1}^i)$, then $\Delta\nu_i(\kappa_t^i - 1) = \cdots = \Delta\nu_i(\kappa) = \cdots = \Delta\nu_i(\kappa_{t-1}^i + 1) = 0$, and $\hat{\omega}_i(\kappa_t^i) = \hat{\omega}_i(\kappa_t^i - 1) = \cdots = \hat{\omega}_i(\kappa) = \cdots = \hat{\omega}_i(\kappa_{t-1}^i)$. Therefore, it can be derived that $\hat{\omega}_i(\kappa)$ is bounded for $\kappa_{t-1}^i \leq \kappa < \kappa_t^i$.

Also, considering $|\Delta\nu_i(\kappa-1)| \leq \alpha$, or $|\omega_i(\kappa)| \leq \alpha$, according to the explanation after Equation (16), we obtain $\hat{\omega}_i(\kappa) = \hat{\omega}_i(1)$ and it is obvious that $\hat{\omega}_i(\kappa)$ is bounded.

Then, substitute the estimation value from Equation (7) into the output estimated error from Equation (6) and combine Equation (2) in Lemma 1, one has

$$\begin{aligned} \varepsilon_i(\kappa+1) &= r_i(\kappa+1) - \hat{r}_i(\kappa+1) \\ &= r_i(\kappa) + \omega_i(\kappa)\Delta\nu_i(\kappa) - \hat{r}_i(\kappa) - \hat{\omega}_i(\kappa)\Delta\nu_i(\kappa_t^i) - Q_i(\hat{r}_i(\kappa) - r_i(\kappa_t^i)) \\ &= r_i(\kappa) - \hat{r}_i(\kappa) + Q_i r_i(\kappa) - Q_i\hat{r}_i(\kappa) - Q_i r_i(\kappa) + \omega_i(\kappa)\Delta\nu_i(\kappa) \\ &\quad - \hat{\omega}_i(\kappa)\Delta\nu_i(\kappa_t^i) - \hat{\omega}_i(\kappa)\Delta\nu_i(\kappa) + \hat{\omega}_i(\kappa)\Delta\nu_i(\kappa) + Q_i r_i(\kappa_t^i) \\ &= (1+Q_i)(r_i(\kappa) - \hat{r}_i(\kappa)) + (\omega_i(\kappa) - \hat{\omega}_i(\kappa))\Delta\nu_i(\kappa) \\ &\quad + \hat{\omega}_i(\kappa)(\Delta\nu_i(\kappa) - \Delta\nu_i(\kappa_t^i)) + Q_i(r_i(\kappa_t^i) - r_i(\kappa)) \\ &= (1+Q_i)\varepsilon_i(\kappa) - \overline{\omega}_i(\kappa)\Delta\nu_i(\kappa) + \hat{\omega}_i(\kappa)(\Delta\nu_i(\kappa) - \Delta\nu_i(\kappa_t^i)) + Q_i(r_i(\kappa_t^i) - r_i(\kappa)). \end{aligned} \tag{28}$$

The following Lyapunov function is devised as below:

$$V_i(\kappa) = (\varepsilon_i(\kappa))^2 \tag{29}$$

At the event-triggered instant, $\kappa = \kappa_t^i$, one has $\Delta\nu_i(\kappa) - \Delta\nu_i(\kappa_t^i) = 0$, $r_i(\kappa_t^i) - r_i(\kappa) = 0$. From Equation (28) one has:

$$\varepsilon_i(\kappa+1) = (1+Q_i)\varepsilon_i(\kappa) - \overline{\omega}_i(\kappa)\Delta\nu_i(\kappa) \tag{30}$$

then, combine Equation (29) and Equation (30), one has

$$\begin{aligned} \Delta V_i(\kappa+1) &= V_i(\kappa+1) - V_i(\kappa) \\ &= (\varepsilon_i(\kappa+1))^2 - (\varepsilon_i(\kappa))^2 \\ &= \left[(1+Q_i)\varepsilon_i(\kappa) - \overline{\omega}_i(\kappa)\Delta\nu_i(\kappa)\right]^2 - (\varepsilon_i(\kappa))^2 \\ &= (1+Q_i)^2(\varepsilon_i(\kappa))^2 - 2(1+Q_i)\varepsilon_i(\kappa)\overline{\omega}_i(\kappa)\Delta\nu_i(\kappa) + (\overline{\omega}_i(\kappa))^2(\Delta\nu_i(\kappa))^2 - (\varepsilon_i(\kappa))^2 \\ &\leq 2(1+Q_i)^2(\varepsilon_i(\kappa))^2 + 2(\overline{\omega}_i(\kappa))^2(\Delta\nu_i(\kappa))^2 - (\varepsilon_i(\kappa))^2 \\ &= (2(1+Q_i)^2 - 1)(\varepsilon_i(\kappa))^2 + 2(\overline{\omega}_i(\kappa))^2(\Delta\nu_i(\kappa))^2 \end{aligned} \tag{31}$$

since $\overline{\omega}_i(\kappa)$ is bounded, and then $2(\overline{\omega}_i(\kappa))^2(\Delta\nu_i(\kappa))^2$ is bounded.

Moreover, define $\varrho_i > 2(\overline{\omega}_i(\kappa))^2(\Delta\nu_i(\kappa))^2$. If $|\varepsilon_i(\kappa)| > \sqrt{\frac{\varrho_i}{1-2(1+Q_i)^2}} = \zeta_i$, $\Delta V_i(\kappa+1) < 0$, then $\varepsilon_i(\kappa)$ is bounded.

During the inter-event time interval, $\kappa_t^i < \kappa < \kappa_{t+1}^i$, according to Equation (28), one has

$$\Delta V_i(\kappa+1) = \left[(1+Q_i)\varepsilon_i(\kappa) + \overline{\omega}_i(\kappa)\Delta\nu_i(\kappa) + \hat{\omega}_i(\kappa)\theta_i(\kappa) + Q_i\rho_i(\kappa)\right]^2 - (\varepsilon_i(\kappa))^2, \tag{32}$$

where $\theta_i(\kappa) = \Delta\nu_i(\kappa) - \Delta\nu_i(\kappa_t^i)$, $\rho_i(\kappa) = r_i(\kappa_t^i) - r_i(\kappa)$, assume that $\rho_i(\kappa)$ is bounded.

For real numbers x and y, it can be obtained that $2xy \leq x^2 + y^2$, then we have

$$2((1+Q_i)\varepsilon_i(\kappa))Q_i\rho_i(\kappa) \leq ((1+Q_i)\varepsilon_i(\kappa))^2 + (Q_i\rho_i(\kappa))^2, \tag{33}$$

$$2((1+Q_i)\varepsilon_i(\kappa))\overline{\omega}_i(\kappa)\Delta\nu_i(\kappa) \leq ((1+Q_i)\varepsilon_i(\kappa))^2 + (\overline{\omega}_i(\kappa)\Delta\nu_i(\kappa))^2, \tag{34}$$

$$2((1+Q_i)\varepsilon_i(\kappa))\hat{\omega}_i(\kappa)\theta_i(\kappa) \leq ((1+Q_i)\varepsilon_i(\kappa))^2 + (\hat{\omega}_i(\kappa)\theta_i(\kappa))^2, \tag{35}$$

$$2(Q_i\rho_i(\kappa))\overline{\omega}_i(\kappa)\Delta\nu_i(\kappa) \leq (Q_i\rho_i(\kappa))^2 + (\overline{\omega}_i(\kappa)\Delta\nu_i(\kappa))^2, \tag{36}$$

$$2(Q_i\rho_i(\kappa))\hat{\omega}_i(\kappa)\theta_i(\kappa) \leq (Q_i\rho_i(\kappa))^2 + (\hat{\omega}_i(\kappa)\theta_i(\kappa))^2, \tag{37}$$

$$2(\overline{\omega}_i(\kappa)\Delta\nu_i(\kappa))\hat{\omega}_i(\kappa)\theta_i(\kappa) \leq (\overline{\omega}_i(\kappa)\Delta\nu_i(\kappa))^2 + (\hat{\omega}_i(\kappa)\theta_i(\kappa))^2. \tag{38}$$

Substitute the inequalities (33)–(38) into Equation (32), one has

$$\begin{aligned}\Delta V_i(\kappa+1) &\leq 4((1+Q_i)\varepsilon_i(\kappa))^2 + 4Q_i(\rho_i(\kappa))^2 + 4(\overline{\omega}_i(\kappa)\Delta\nu_i(\kappa))^2 + 4(\hat{\omega}_i(\kappa)\theta_i(\kappa))^2 - (\varepsilon_i(\kappa))^2 \\ &= 4(1+Q_i)^2(\varepsilon_i(\kappa))^2 - (\varepsilon_i(\kappa))^2 + 4Q_i^2(\rho_i(\kappa))^2 + 4(\overline{\omega}_i(\kappa))^2(\Delta\nu_i(\kappa))^2 + 4(\hat{\omega}_i(\kappa))^2(\theta_i(\kappa))^2 \\ &= (4(1+Q_i)^2 - 1)(\varepsilon_i(\kappa))^2 + 4(\hat{\omega}_i(\kappa))^2(\theta_i(\kappa))^2 + 4Q_i^2(\rho_i(\kappa))^2 + 4(\overline{\omega}_i(\kappa))^2(\Delta\nu_i(\kappa))^2 \\ &= (4(1+Q_i)^2 - 1)(\varepsilon_i(\kappa))^2 + 4Q_i^2(r_i(\kappa_t^i) - r_i(\kappa))^2 + \Omega_i(\kappa),\end{aligned} \tag{39}$$

where $\Omega_i(\kappa) = 4(\hat{\omega}_i(\kappa))^2(\theta_i(\kappa))^2 + 4(\overline{\omega}_i(\kappa))^2(\Delta\nu_i(\kappa))^2$ and $\Omega_i(\kappa)$ is bounded.

Moreover, there exists $0 < \gamma < 1$, which satisfies

$$4Q_i^2(r_i(\kappa_t^i) - r_i(\kappa))^2 \leq \gamma(1 - 4(1+Q_i)^2)(\varepsilon_i(\kappa))^2$$

then

$$\left|r_i(\kappa_t^i) - r_i(\kappa)\right| \leq \frac{\sqrt{\gamma(1-4(1+Q_i)^2)}}{2|Q_i|}|\varepsilon_i(\kappa)|. \tag{40}$$

Furthermore, one can get

$$\begin{aligned}\Delta V_i(\kappa+1) &\leq (4(1+Q_i)^2 - 1)(\varepsilon_i(\kappa))^2 + \gamma(1 - 4(1+Q_i)^2)(\varepsilon_i(\kappa))^2 + \Omega_i(\kappa) \\ &= (\gamma - 1)(1 - 4(1+Q_i)^2)(\varepsilon_i(\kappa))^2 + \Omega_i(\kappa).\end{aligned} \tag{41}$$

One has $0 < 1 - 4(1+Q_i)^2 < 1$ by choosing the proper parameter Q_i, then from the inequality (41) one obtains

$$\begin{aligned}V_i(\kappa+1) &\leq V_i(\kappa) + (\gamma - 1)(1 - 4(1+Q_i)^2)(\varepsilon_i(\kappa))^2 + \Omega_i(\kappa) \\ &= \Phi_i V_i(\kappa) + \Omega_i(\kappa) \\ &\leq \Phi_i(\Phi_i V_i(\kappa-1) + \Omega_i(\kappa)) + \Omega_i(\kappa) \\ &\leq \cdots \\ &\leq \Phi_i^\kappa V_i(1) + (\Phi_i^{\kappa-1} + \Phi_i^{\kappa-2} + \cdots + \Phi_i + 1)\Omega_i(\kappa) \\ &= \Phi_i^\kappa V_i(1) + \frac{1 - \Phi_i^\kappa}{1 - \Phi_i}\Omega_i(\kappa),\end{aligned} \tag{42}$$

where $\Phi_i = 1 + (\gamma - 1)(1 - 4(1 + Q_i)^2)$ and $0 < \Phi_i < 1$, therefore, $V_i(\kappa + 1)$ is bounded and it can be derived that $\varepsilon_i(\kappa)$ is also bounded. Then the proof of Theorem 1 is completed. ■

In Theorem 1, the PPD estimation $\hat{\omega}_i(\kappa)$ and the output estimated error $\varepsilon_i(\kappa)$ are verified to be bounded by taking two cases into consideration. One case is at the event-triggered instant $\kappa = \kappa_t^i$, the other is between the triggering interval, that is, $\kappa_t^i < \kappa < \kappa_{t+1}^i$. In the next theorem, the tracking error $o_i(\kappa) = r_d(\kappa) - r_i(\kappa)$ is proved to be convergent based on Theorem 1. Therefore, all the agents of the MAS can track the desired trajectory.

Theorem 2. *If Assumptions 1 and 2 are satisfied, the desired trajectory $r_d(\kappa)$ is time-invariable and $0 < \frac{b}{2\sqrt{\lambda}} < 1$, then the tracking error $o_i(\kappa)$ is convergent.*

Proof. From Equation (4), the combined measurement error $\psi_i(\kappa)$ can be rewritten as follows:

$$\psi_i(\kappa) = \sum_{j \in N_i(\kappa)} a_{j,i}(\kappa)(o_i(\kappa) - o_j(\kappa)) + d_i(\kappa)o_i(\kappa). \tag{43}$$

Moreover, define the following column vectors:

$$\begin{aligned} \tilde{o}(\kappa) &= [o_1(\kappa), o_2(\kappa), \dots, o_N(\kappa)]^T \\ \tilde{\psi}(\kappa) &= [\psi_1(\kappa), \psi_2(\kappa), \dots, \psi_N(\kappa)]^T \\ \tilde{r}(\kappa) &= [r_1(\kappa), r_2(\kappa), \dots, r_N(\kappa)]^T \\ \tilde{v}(\kappa) &= [v_1(\kappa), v_2(\kappa), \dots, v_N(\kappa)]^T. \end{aligned}$$

Then, from Equation (43) we have

$$\tilde{\psi}(\kappa) = (\mathcal{M}(\kappa) + \mathcal{D}(\kappa))\tilde{o}(\kappa) \tag{44}$$

where $\mathcal{M}(\kappa)$ and $\mathcal{D}(\kappa)$ are introduced in the previous section.

Based on Equation (44), Equation (19) can be rewritten as

$$\begin{aligned} \tilde{v}(\kappa) &= \tilde{v}(\kappa - 1) + \rho F_1(\kappa)\tilde{\psi}(\kappa) \\ &= \tilde{v}(\kappa - 1) + \rho F_1(\kappa)(\mathcal{M}(\kappa) + \mathcal{D}(\kappa))\tilde{o}(\kappa) \end{aligned} \tag{45}$$

where $F_1(\kappa) = diag(\frac{\hat{\omega}_1(\kappa-1)}{\lambda+\hat{\omega}_1(\kappa-1)^2}, \frac{\hat{\omega}_2(\kappa-1)}{\lambda+\hat{\omega}_2(\kappa-1)^2}, \dots, \frac{\hat{\omega}_N(\kappa-1)}{\lambda+\hat{\omega}_N(\kappa-1)^2})$.

Similarly, from Equation (2), we can obtain that

$$\tilde{r}(\kappa + 1) = \tilde{r}(\kappa) + F_2(\kappa)\Delta\tilde{v}(\kappa), \tag{46}$$

where $F_2(\kappa) = diag(\omega_1(\kappa), \omega_2(\kappa), \dots, \omega_N(\kappa))$, $\Delta\tilde{v}(\kappa) = \tilde{v}(\kappa) - \tilde{v}(\kappa - 1)$.

Since $r_d(\kappa)$ is time-invariable, combine Equation (45) and Equation (46) we have

$$\begin{aligned} \tilde{o}(\kappa + 1) &= \tilde{o}(\kappa) - \rho F_1(\kappa)F_2(\kappa)(\mathcal{M}(\kappa) + \mathcal{D}(\kappa))\tilde{o}(\kappa) \\ &= (I - \rho F_3(\kappa)(\mathcal{M}(\kappa) + \mathcal{D}(\kappa)))\tilde{o}(\kappa), \end{aligned} \tag{47}$$

where $F_3(\kappa) = F_1(\kappa)F_2(\kappa) = diag(\frac{\omega_1(\kappa)\hat{\omega}_1(\kappa-1)}{\lambda+\hat{\omega}_1(\kappa-1)^2}, \frac{\omega_2(\kappa)\hat{\omega}_2(\kappa-1)}{\lambda+\hat{\omega}_2(\kappa-1)^2}, \dots, \frac{\omega_N(\kappa)\hat{\omega}_N(\kappa-1)}{\lambda+\hat{\omega}_N(\kappa-1)^2})$.

From Theorem 1, since $\hat{\omega}_i(\kappa)$ and $\omega_i(\kappa)$ are bounded for $i = 1, 2, \dots, N$, we can derive that

$$0 < \frac{\omega_i(\kappa)\hat{\omega}_i(\kappa - 1)}{\lambda + \hat{\omega}_i(\kappa - 1)^2} \le \frac{b\hat{\omega}_i(\kappa - 1)}{2\sqrt{\lambda}|\hat{\omega}_i(\kappa - 1)|} \le \frac{b}{2\sqrt{\lambda}} < 1. \tag{48}$$

From the Equation (47) and Equation (48), we can obtain that if $\|I - \rho F_3(\kappa)(\mathcal{M}(\kappa) + \mathcal{D}(\kappa))\| < 1$, then $\lim_{\kappa\to\infty} \|\tilde{o}(\kappa + 1)\| = 0$, that is, the tracking error $o(\kappa)$ converges to 0.

This completes the proof of Theorem 2. ∎

Remark 7. Different from References 11 and 12, in this article, an event-triggered mechanism is established to solve the problem of the constraint of network bandwidth, and an attack compensation mechanism is considered to mitigate the alleviate of DoS attacks. The tracking control problem investigated in this article is influenced by both the event-triggered mechanism and DoS attacks. Moreover, unlike the method in Reference 32, the consensus control issue for data-driven MASs is investigated based on switching topologies rather than fixed topologies.

4 | SIMULATION EXAMPLE

This section provides a simulation example to illustrate the effectiveness of the ETMFAC consensus tracking strategy with the attack compensation mechanism.

Consider a heterogeneous nonlinear MAS comprising four follower agents. Since the communication graphs of the MAS switch among three states, the directed graphs of the system are chosen in $\mathcal{T}(\kappa) = \{\mathcal{T}_1, \mathcal{T}_2, \mathcal{T}_3\}$ which are shown in Figure 2. A random switching signal $\delta(\kappa)$ is introduced that switches randomly from $\{1, 2, 3\}$, that is, one of the three predefined topologies in Figure 2 is selected by using the signal function $\delta(\kappa)$.

The desired trajectory is presented as:

$$r_d(\kappa) = \begin{cases} 2, & 0 < \kappa < 400, \\ 0.3, & 400 \leq \kappa < 800. \end{cases}$$

The dynamics of the four agents are given as follows:

$$\begin{aligned} r_1(\kappa+1) &= \frac{r_1(\kappa)v_1(\kappa)}{1 + r_1(\kappa)^2} + v_1(\kappa), \\ r_2(\kappa+1) &= \frac{(r_2(\kappa) + 0.05)v_2(\kappa)}{1 + r_2(\kappa)^3} + 0.5v_2(\kappa), \\ r_3(\kappa+1) &= \frac{r_3(\kappa)v_3(\kappa)}{1 + r_3(\kappa)^2} + 0.9v_3(\kappa), \\ r_4(\kappa+1) &= \frac{r_4(\kappa)v_4(\kappa)}{1 + r_4(\kappa)^3} + 0.8v_4(\kappa). \end{aligned}$$

In this simulation example, the dynamics above are only utilized to generate the I/O data of agents rather than the specific model in the proposed ETMFAC approach.

The initial values of the system are given as $v_i(1) = 0$, $\hat{\omega}_i(1) = 2$ and $r_1(1) = 0.4$, $r_2(1) = 2.6$, $r_3(1) = 3.3$, $r_4(1) = 3.9$. Other parameters are chosen as $\alpha = 10^{-5}$, $\eta = 1$, $\rho = 0.3$, $\lambda = 0.85$, $\gamma = 0.5$ and $\beta_i = 0.5$. To make the simulation more convenient, we define $Q_i = -0.500015$.

The combined measurement error $\psi_i(\kappa)$ in Equation (3) can be obtained based on the selected communication topology. Then, the PPD estimation value $\hat{\omega}_i(\kappa)$ and the system input $v_i(\kappa)$ can be derived based on Equation (16) and

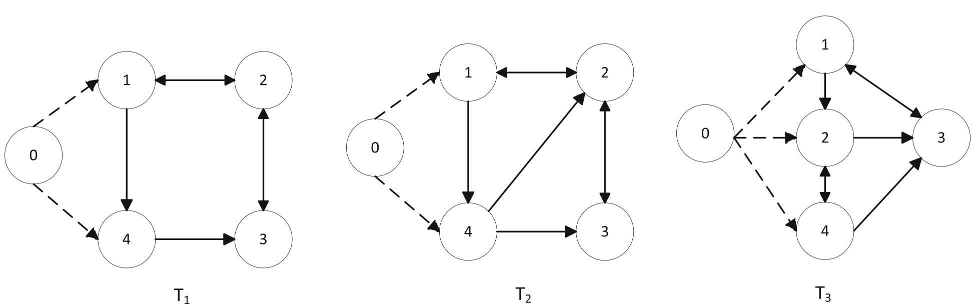

FIGURE 2 The communication topologies.

(19). Furthermore, the tracking error $o_i(\kappa)$ is obtained combing system (1) and Equation (21). From the conclusion in Theorem 2, since $o_i(\kappa)$ is bounded, the outputs of the four agents tend to overlap with the tracking trajectory $r_d(\kappa)$ over time and the tracking errors can converge to 0.

The tracking performance for the desired trajectory subject to DoS attacks is shown in Figure 3, and the tracking errors are illustrated in Figure 4. From Figure 3, we can obtain that although the output curves of each agent are initially fluctuating, they can eventually coverage to the desired trajectory. From Figure 4, it can be derived that there exist large

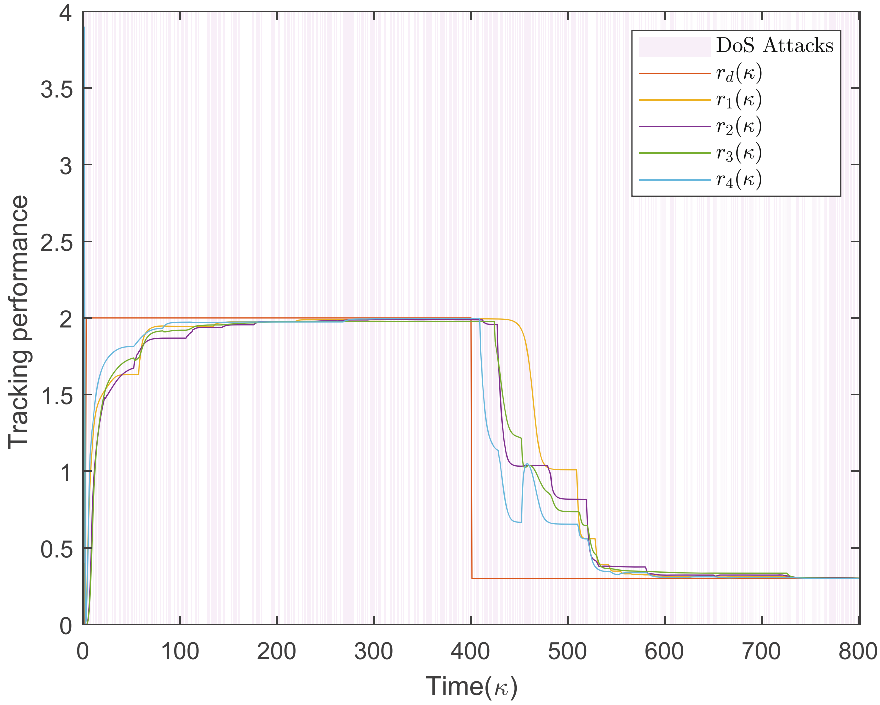

FIGURE 3 Tracking performance for the desired trajectory under DoS attacks.

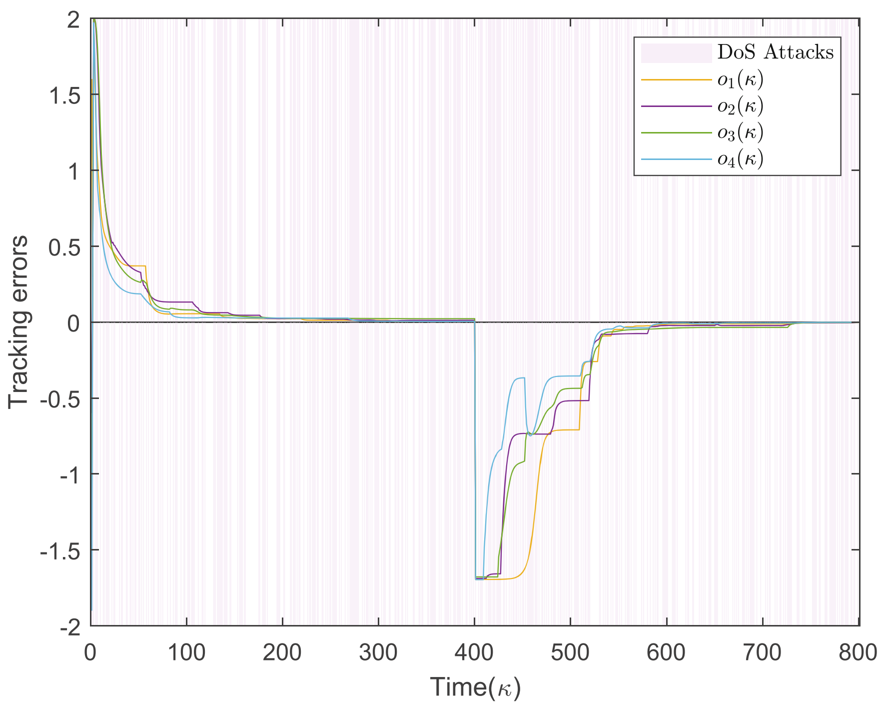

FIGURE 4 Consensus tracking errors for the desired trajectory under DoS attacks.

deviations between the followers' outputs and the desired output at first, then, the tracking errors reduce rapidly and finally converge to 0. The stochastic switching signal $\delta(\kappa)$ is shown in Figure 5. Moreover, the input signals of all agents are presented in Figure 6, and Figure 7 presents the event-triggered instants of all agents. From Figures 6 and 7, it can be obtained that as the input signal of the controller stabilizes, the system has fewer event-triggered instants.

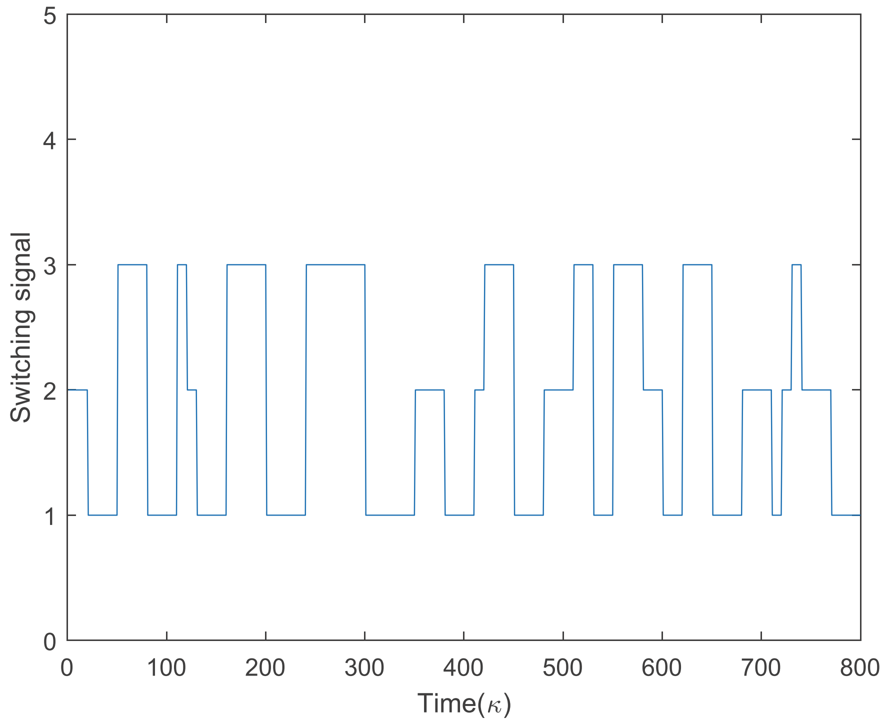

FIGURE 5 The stochastic switching signal of the three communication graphs.

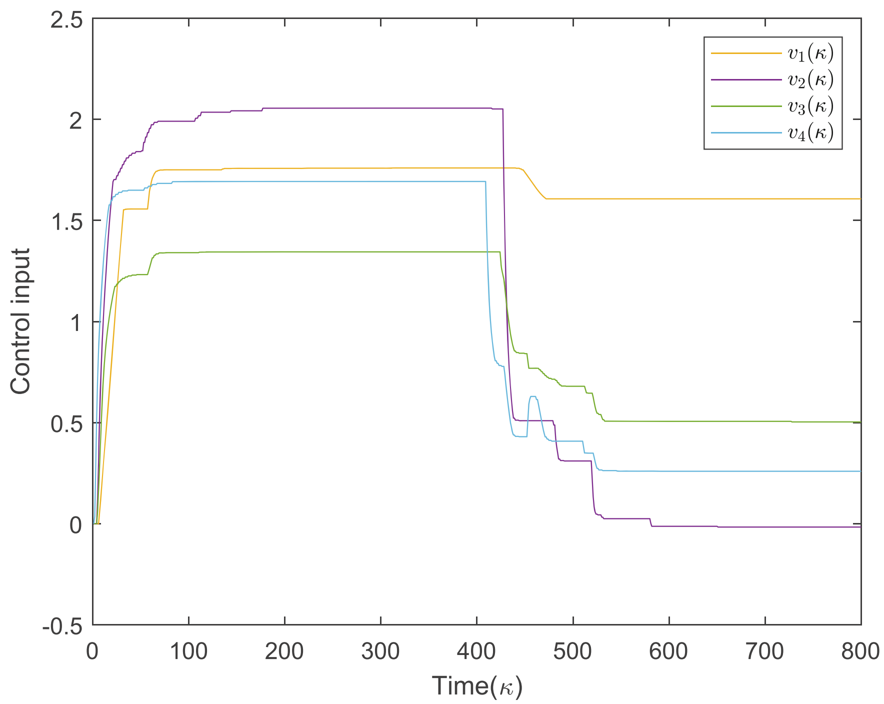

FIGURE 6 Input signals of all agents.

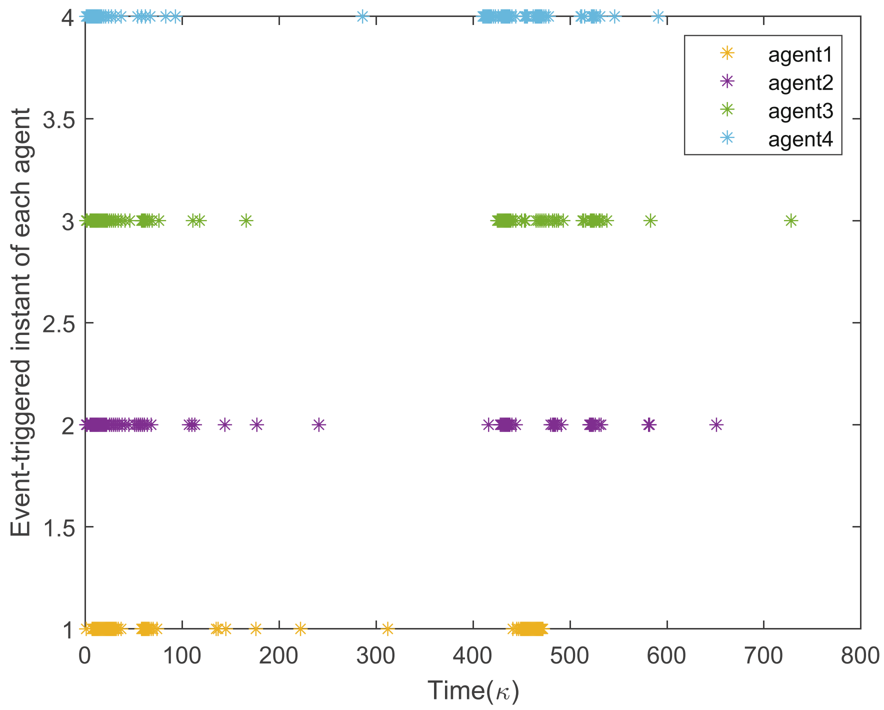

FIGURE 7 Event-triggered instants of all agents.

5 | CONCLUSION

This article has studied the consensus tracking control for nonlinear MASs with switching topologies subject to DoS attacks by using a proposed ETMFAC approach. First, the system model has been dynamically linearized on the basis of PPD. Next, an event-triggered scheme has been adopted to address the problem of bandwidth limitation. Then, an attack compensation mechanism has been given to reduce the impact of DoS attacks. Furthermore, the MFAC-based controller has been designed without any information of the unknown model and only the I/O measurement of agents is required. Finally, a simulation example has been provided to testify the validity of the developed ETMFAC approach.

FUNDING INFORMATION

This work was supported by the National Natural Science Foundation of China under Grant 62373252, Grant 62273174, and Grant 61903182, in part by the Natural Science Foundation of Jiangsu Province of China under Grant BK20230063 and Startup Foundation for Introducing Talent of NUIST under Grant 2024r063.

CONFLICT OF INTEREST STATEMENT

The authors declare no conflicts of interest.

DATA AVAILABILITY STATEMENT

The data that support the findings of this study are available on request from the corresponding author. The data are not publicly available due to privacy or ethical restrictions.

ORCID

Jinliang Liu https://orcid.org/0000-0001-5489-0246
Lijuan Zha https://orcid.org/0000-0003-0475-8866
Engang Tian https://orcid.org/0000-0002-8169-5347
Xiangpeng Xie https://orcid.org/0000-0003-4822-3134

REFERENCES

1. Tang Y, Xing X, Karimi HR, Kocarev L, Kurths J. Tracking control of networked multi-agent systems under new characterizations of impulses and its applications in robotic systems. *IEEE Trans Ind Electron*. 2016;63(2):1299-1307.
2. Dong X, Hua Y, Zhou Y, Ren Z, Zhong Y. Theory and experiment on formation-containment control of multiple multirotor unmanned aerial vehicle systems. *IEEE Trans Autom Sci Eng*. 2019;16(1):229-240.
3. Karkoub M, Wang H, Wu T. Distributed Newton and Quasi-Newton methods for formation control of autonomous vehicles. *Ships Offshore Struct*. 2020;15(1):61-74.
4. Li H, Xie L, Zhang X, Pan W. Distributed consensus control of nonlinear multi-agent systems with sensor uncertainty. *Int J Robust Nonlinear Control*. 2023;33:973-990.
5. Luo S, Xu J, Liang X. Mean square consensus of heterogeneous multi-agent systems with time-varying communication delays and intermittent observations. *IEEE Trans Circuits Syst II Exp Briefs*. 2022;69(1):184-188.
6. Tang Y, Zhu K. Optimal consensus for uncertain high-order multi-agent systems by output feedback. *Int J Robust Nonlinear Control*. 2022;32:2084-2099.
7. Zhang X, Wang G, Sun J. Data-driven control of consensus tracking for discrete-time multi-agent systems. *J Franklin Inst*. 2023;360(7):4661-4674.
8. Liang M, Li J. Distributed data-driven iterative learning point-to-point consensus tracking control for unknown nonlinear multi-agent systems. *Neurocomputing*. 2023;561:126875.
9. Xu K, Meng B, Wang Z. Design of data-driven mode-free iterative learning controller based higher order parameter estimation for multi-agent systems consistency tracking. *Knowl-Based Syst*. 2023;261:110221.
10. Bu X, Hou Z, Zhang H. Data-driven multi-agent systems consensus tracking using model free adaptive control. *IEEE Trans Neural Networks Learn Syst*. 2018;29(5):1514-1524.
11. Zhao H, Li P, Yu H. Model-free adaptive consensus tracking control for unknown nonlinear multi-agent systems with sensor saturation. *Int J Robust Nonlinear Control*. 2021;31(13):1146-1155.
12. Hou Z, Xiong S. On model-free adaptive control and its stability analysis. *IEEE Trans Autom Control*. 2019;64(11):4555-4569.
13. Zhang Z, Lunze J, Sun Y, Lu Z. Dynamic event-triggered communication based distributed optimization. *Int J Robust Nonlinear Control*. 2021;31(17):419-421.
14. Nowzari C, Garcia E, Cortés J. Event-triggered communication and control of networked systems for multi-agent consensus. *Automatica*. 2019;105:1-27.
15. Zhu Q. Stabilization of stochastic nonlinear delay systems with exogenous disturbances and the event-triggered feedback control. *IEEE Trans Autom Control*. 2019;64(9):3764-3771.
16. Zhang L, Deng C, An L. Asymptotic tracking control of nonlinear strict-feedback systems with state/output triggering: a homogeneous filtering approach. *IEEE Trans Autom Control*. 2024. doi:10.1109/TAC.2024.3383090
17. Zhang L, Deng C, Che W, An L. Adaptive backstepping control for nonlinear interconnected systems with prespecified-performance-driven output triggering. *Automatica*. 2023;154:111063.
18. Huang J, Jia W, Wan T, Xiao S, Wang L, Dong J. Adaptive event-triggered fault-tolerant consensus of linear heterogeneous multiagent systems via hierarchical approach. *Appl Math Comput*. 2023;447:127909.
19. Du S, Sheng H, Sun H. A fully distributed event-triggered control approach to leader-following consensus of multiagent systems. *J Franklin Inst*. 2023;360(17):13227-13243.
20. Zhang J, Tong S. Dynamic event-triggered adaptive NN consensus control for nonlinear multiagent systems with unknown measurement sensitivity. *Neurocomputing*. 2023;560:126854.
21. Ren H, Liu R, Cheng Z, Ma H, Li H. Data-driven event-triggered control for nonlinear multi-agent systems with uniform quantization. *IEEE Trans Circuits Syst II Exp Briefs*. 2024;71(2):712–716.
22. Liu Z, Shi Y, Yan H, Han B, Guan Z. Secure consensus of multiagent systems via impulsive control subject to deception attacks. *IEEE Trans Circuits Syst II Exp Briefs*. 2023;70(1):166-170.
23. Li S, Zou W, Guo J, Xiang Z. Consensus of switched nonlinear multiagent systems subject to cyber attacks. *IEEE Syst J*. 2022;16(3):4423-4432.
24. Zhang D, Feng G. A new switched system approach to leader–follower consensus of heterogeneous linear multi-agent systems with DoS attack. *IEEE Trans Syst Man Cybern Syst*. 2021;51(2):1258-1266.
25. Huang X, Dong J. Reliable leader-to-follower formation control of multi-agent systems under communication quantization and attacks. *IEEE Trans Syst Man Cybern Syst*. 2020;50(1):89-99.
26. Liu J, Dong Y, Zha L, Xie X, Tian E. Reinforcement learning-based tracking control for networked control systems with DoS attacks. *IEEE Trans Inf Forensics Secur*. 2024;19:4188-4197.
27. Du S, Yan Q, Dong L, Qiao J. Secure consensus of multi-agent systems with input saturation and distributed multiple DoS attacks. *IEEE Trans Circuits Syst II Exp Briefs*. 2022;69(4):2246-2250.
28. Deng C, Wen C. Distributed resilient observer-based fault-tolerant control for heterogeneous multi-agent systems under actuator faults and DoS attacks. *IEEE Trans Control Netw Syst*. 2020;7(3):1308-1318.
29. Zhao H, Niu Y, Zhao J. Event-triggered sliding mode control of uncertain switched systems under denial-of-service attacks. *J Franklin Inst*. 2019;356(18):11414-11433.
30. Cheng T, Kan Z, Klotz JR, Shea JM, Dixon WE. Event-triggered control of multi-agent systems for fixed and time-varying network topologies. *IEEE Trans Autom Control*. 2017;62(10):5365-5371.

31. Zou W, Zhou C, Guo J, Xiang Z. Global adaptive leader-following consensus for second-order nonlinear multiagent systems with switching topologies. *IEEE Trans Circuits Syst II Exp Briefs*. 2021;68(2):702-706.
32. Lu R, Wu J, Zhan X, Yan H. Finite-time bipartite consensus for second-order nonlinear multi-agent systems under random switching topologies. *IEEE Trans Circuits Syst II Exp Briefs*. 2023;70(12):4474-4478.
33. Jiang J, Jiang Y. Leader-following consensus of multi-agent systems under fixed and switching topologies. *Syst Control Lett*. 2010;59:209-217.
34. Liu D, Liu N, Li T. Event-triggered model-free adaptive control for nonlinear systems with output saturation. *Int J Robust Nonlinear Control*. 2023;33(12):7204-7220.
35. Xiong S, Hou Z, Jin S. Model-free adaptive formation control for unknown multiinput-multioutput nonlinear heterogeneous discrete-time multiagent systems with bounded disturbance. *Int J Robust Nonlinear Control*. 2020;30(15):6330-6350.
36. Zha L, Liao R, Liu J, Xie X, Tian E, Cao J. Outlier-resistant distributed filtering over sensor networks under dynamic event-triggered schemes and DoS attacks. *IEEE Trans Autom Sci Eng*. doi:10.1109/TASE.2024.3360718
37. Wu Z, Zhang L, Yue M. Low-rate DoS attacks detection based on network multifractal. *IEEE Trans Depend Secure Comput*. 2016;13(5):559-567.
38. Hou Z, Jin S. A novel data-driven control approach for a class of discrete-time nonlinear systems. *IEEE Trans Control Syst Technol*. 2011;19(6):1549-1558.

How to cite this article: Liu J, Liu Y, Zha L, Tian E, Xie X. Event-triggered consensus tracking strategy for data-driven multi-agent systems under DoS attacks. *Int J Robust Nonlinear Control*. 2024;34(15):10666-10682. doi: 10.1002/rnc.7535